Reliability-based Precancellation of Inter-Carrier Interference for Highly Mobile OFDM Systems

Rana Desouky Kazamel
Institute of Telecommunications
Stuttgart University

Nabil Sven Loghin
European Technology Center
Sony Stuttgart

Joachim Speidel
Institute of Telecommunications
Stuttgart University

***Abstract*—Orthogonal Frequency Division Multiplexing (OFDM) systems in fast time-varying channels suffer from inter-carrier interference (ICI), which necessitates the use of ICI mitigating equalizers. The performance of the equalizers strongly depends on the channel estimation (CE). Estimating the channel matrix in the frequency domain using pilot estimates can only provide limited performance, because pilots are also corrupted by ICI. We propose two approaches for reliability-based ICI precancellation at the receiver to improve CE. Firstly, a log-likelihood ratio window is used to optimize the interpolation points for CE. Secondly, a post-processor is employed to improve the estimates of the pilots' neighbours. The low-complexity minimum mean squared error decision feedback frequency equalizer, which exploits the banded structure of the channel matrix, showed increased performance gains after both proposed ICI precancellation schemes.**

I. Introduction

OFDM is widely used in high speed communication systems due to its robustness against frequency selective fading, simple transceiver structure and high spectral efficiency. One of the main advantages of OFDM is simple equalization, because it renders the frequency selective channel to a flat fading channel at each subcarrier, enabling the use of a one-tap frequency equalizer (FEQ). However, since the channel can vary within one OFDM symbol, the orthogonality between the subcarriers is destroyed due to ICI. As a result, a one-tap FEQ is no longer sufficient. ICI also arises due to carrier frequency offsets and timing synchronization errors at the receiver. The effect of ICI becomes more severe as the normalized Doppler frequency increases, which is given by $f_{dnorm} = \frac{f_c v}{c\Delta f}$, where f_c is the carrier frequency, Δf is the subcarrier spacing, v is the velocity and c is the speed of light. As a result, to support higher mobility, for example in trains or on highways, and to use larger FFT sizes, ICI mitigation is essential.

Several techniques have been proposed in the literature including linear FEQs based on minimum mean squared error (MMSE) or zero-forcing (ZF) detectors [1]-[5], and non-linear FEQs based on decision feedback or ICI cancellation [1], [2], [6], where the non-linear FEQs outperform the linear ones. The performance of ICI mitigating FEQs strongly depends on the channel matrix estimation accuracy. The number of unknown channel taps needed to estimate the matrix are much larger than the number of observations; therefore, the channel's time variation (CTV) needs to be modeled [3], [7]. A polynomial was used to model the CTV in [7], and even a polynomial of degree one showed reasonable performance at moderate signal-to-noise ratio (SNR) values.

The resulting linear time varying (LTV) channel model was investigated in [8], and is one of the most promising approaches. However, a great degradation in performance results from the ICI-corrupted pilot estimates used for CE. As a solution, ICI precancellation at the pilots was proposed in [6], using the estimated channel of the previous two OFDM symbols to model the ICI effect and a one-tap FEQ to get initial symbol estimates. This ICI precancellation approach suffers as f_{dnorm} increases for two reasons. Firstly, for fast time-varying channels, the CTV at the current OFDM symbol can not be modeled by the previous two OFDM symbols, as the channel might have severly changed since the last two symbols. Secondly, using the estimates of the one-tap FEQ leads to error propagation (EP) due to wrong ICI precancellation. Thus, in this paper, the previous, current, and next OFDM symbols are used to model the CTV. Although the ICI-corrupted pilots are used for CE at the current and next OFDM symbols, they can better represent the CTV. To mitigate the effect of EP two approaches will be introduced: a reliability-based log-likelihood ratio (LLR) window used to optimize the interpolation points (IPs) for CE and a post-processor (PP) to improve the estimates of the pilots' neighbours.

This paper is organized as follows. Section II introduces the system model. The optimal 1D Wiener CE in the frequency direction is discussed in section III, followed by the linear MMSE FEQ and non-linear decision feedback equalizer (DFE) in section IV. Section V presents the ICI precancellation approaches. The results are then explained in section VI. Finally, the conclusions are discussed in section VII.

II. System Model

We consider an OFDM system with N subcarriers over a doubly selective Rayleigh fading wide sense stationary uncorrelated scattering channel, assuming Jakes' power spectral density. At the transmitter, each $log_2 M$ bits are mapped into a symbol with M-ary quadrature amplitude modulation (M-QAM). The M-QAM symbols are then converted to the time domain (TD) by the N-point inverse fast Fourier transform (IFFT). The TD signal $x(n)$ is given by

$$x(n) = \frac{1}{\sqrt{N}} \sum_{k=0}^{N-1} X_k e^{\frac{j2\pi kn}{N}} \quad 0 \leq n \leq N-1 \,, \qquad (1)$$

978-1-4673-0990-5/12/$31.00 ©2012 IEEE

where X_k is the frequency domain (FD) symbol at subcarrier k. Afterwards, a cyclic prefix (CP) of size N_{CP}, greater than the channel's maximum delay L, is added to avoid inter-symbol interference. The received signal is expressed as

$$y(n) = \sum_{l=0}^{L-1} h(n,l)x(n-l) + w(n) \ , \tag{2}$$

where $h(n,l)$ is the l^{th} path at time instant n and $w(n)$ is the additive white Gaussian noise (AWGN) with zero mean and variance σ^2_{AWGN}. After removing the CP and applying the FFT, the received signal at subcarrier k is

$$Y_k = \frac{1}{N}\sum_{n=0}^{N-1}\sum_{l=0}^{L-1}\sum_{k'=0}^{N-1} X_{k'}h(n,l)e^{\frac{j2\pi(n-l)k'}{N}}e^{-\frac{j2\pi nk}{N}} + W_k \ , \tag{3}$$

where W_k is the AWGN at subcarrier k. In short-hand matrix notation, (3) can be expressed as

$$Y = HX + W \ , \tag{4}$$

where H is the NxN FD channel matrix with entries

$$H_{k,k'} = \frac{1}{N}\sum_{n=0}^{N-1}\sum_{l=0}^{L-1} h(n,l)e^{-\frac{j2\pi k'l}{N}}e^{\frac{j2\pi(k'-k)n}{N}} \ . \tag{5}$$

The main diagonal of the channel matrix ($k' = k$) is

$$H_{k,k} = \sum_{l=0}^{L-1} h^{ave}(l)e^{-\frac{j2\pi kl}{N}} \ , \tag{6}$$

where $h^{ave}(l) = \frac{1}{N}\sum_{n=0}^{N-1} h(n,l)$ is the average value of channel tap l over the N time instants. For a time invariant channel within one OFDM symbol, H becomes a diagonal matrix and there is no ICI. For a fast time-varying channel, H has a banded structure given by H^{banded} in Fig. 1, since the strongest interference comes from the neighbouring subcarriers [2].

III. Channel Matrix Estimation

A. Main Diagonal Estimation

The main diagonal of the channel matrix is estimated using the 1D Wiener filter in the frequency direction. The least squares (LS) estimates of the channel frequency response (CFR) at pilot position $p \in P$ is

$$\hat{H}_{p,p} = \frac{Y_p}{X_p} = H_{p,p} + \frac{I_p + W_p}{X_p} \ , \tag{7}$$

where P is the set of pilot indices and I_p is the total ICI at pilot p. The CFR is then estimated at the data subcarriers using Wiener interpolation based on the LS estimates

$$\hat{H}_{k,k} = \sum_{p\in P} w_0(k,p)\hat{H}_{p,p} \ , \tag{8}$$

where $w_0(k,p)$ is the Wiener filter coefficient corresponding to pilot p. To reduce the complexity only the closest N_{taps} pilots are used to calculate the filter coefficients.

The filter coefficients depend on the autocorrelation of the CFR R in the frequency direction and are given by

$$w_o(k,P) = R^{-1}_{H_P,H_P}R_{k,H_P} \ , \tag{9}$$

where $R_{H_PH_P}$ is the autocorrelation of the CFR at the N_{taps} pilot positions and R_{k,H_P} is the crosscorrelation of the CFR at subcarrier k and the N_{taps} pilot positions.

$$R_{H_P,H_P} = \begin{bmatrix} R(0)+\sigma^2 & \dots & R(p_1 - p_{N_{taps}}) \\ \vdots & \vdots & \vdots \\ R(p_{N_{taps}} - p_1) & \dots & R(0)+\sigma^2 \end{bmatrix} \tag{10}$$

$$R_{k,H_P} = [R(k-p_1) \ \dots \ R(k-p_{N_{taps}})]^T \ , \tag{11}$$

where $R(n-m) = E[H_{n,n}H^*_{m,m}]$ and $\sigma^2 = \sigma^2_{AWGN} + \sigma^2_{ICI}$ is the noise plus ICI power. σ^2_{ICI} is computed by [1, eq.(15)].

B. Off-diagonals Estimation

To compute the channel matrix, the NxL channel taps are required. The LTV model can effectively be used up to f_{dnorm} of 20%, where the average power of the difference in the autocorrelations of Jakes' and the LTV models is almost 3% [8]. With the LTV model, $h(n,l)$ is approximated by

$$h(n,l) = h(\frac{N-1}{2},l) + \Delta h(n,l) \tag{12}$$

$$\Delta h(n,l) = \begin{cases} \left(n - \frac{N-1}{2}\right)\alpha(l,1) & 0 \le n < \frac{N}{2} \\ \left(n - \frac{N-1}{2}\right)\alpha(l,2) & \frac{N}{2} \le n \le N-1 \ , \end{cases} \tag{13}$$

where $\alpha(l,1)$ and $\alpha(l,2)$ are the slopes of the l^{th} channel tap in the first and second half of the OFDM symbol, respectively, and $\Delta h(n,l)$ denotes the deviation of $h(n,l)$ from $h(\frac{N-1}{2},l)$. All time instants are expressed with respect to the midpoint of the OFDM symbol, because the pilot-estimated $h^{ave}(l)$ is approximated by $h(\frac{N-1}{2},l)$, since $E[|h^{ave}(l) - h(s,l)|^2]$ is minimized for $s = \frac{N-1}{2}$ [8].

$\alpha(l,1)$ and $\alpha(l,2)$ are used to estimate the channel taps' variations within the OFDM symbol using the previous and next OFDM symbols and are given respectively by [8]

$$\alpha(l,1) = \frac{h^{ave}_t(l) - h^{ave}_{t-1}(l)}{N+N_{CP}} \tag{14}$$

$$\alpha(l,2) = \frac{h^{ave}_{t+1}(l) - h^{ave}_t(l)}{N+N_{CP}} \ , \tag{15}$$

where t is the OFDM symbol index. The off-diagonals are computed by substituting (12) and (13) into (5) for $k = k' + d$ given by [4, eq.(17)]. After Wiener CE, instead of going back to the TD to estimate the off-diagonal elements, the slopes can be estimated in the FD with respect to the subcarriers.

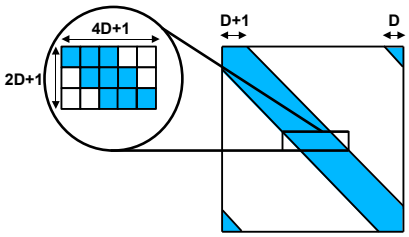

Fig. 1. Structure of H^{banded}

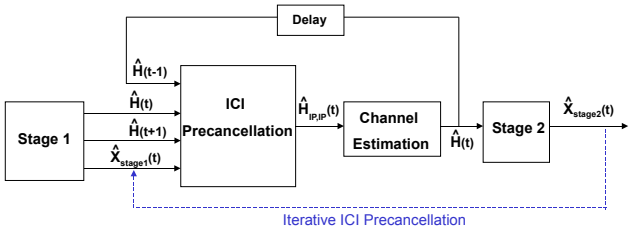

Fig. 2. Two-stage equalizer with a feedback loop

IV. Equalizers

A. Minimum Mean Squared Error Equalizer

The MMSE equalizer estimates are given by

$$\tilde{X} = (H^H H + \sigma^2_{AWGN} I_N)^{-1} H^H Y \ , \qquad (16)$$

where I_N is the NxN identity matrix and $(.)^H$ denotes the Hermitian operator. Computing the MMSE estimates using (16) requires inverting an NxN matrix, which has a complexity of $O(N^3)$. However, the complexity can be significantly reduced by making use of H^{banded} whose non-zero elememts are $2D+1$ diagonals and two DxD upper-right and lower-left triangles coming from the periodic repetition of the spectrum. The symbols can be estimated sequentially by breaking down H^{banded} to smaller matrices of size $(2D+1)$x$(4D+1)$ [2]. The MMSE estimate at subcarrier k is now given by

$$\tilde{X}_k = h^H_{sub,k}(H_{sub,k} H^H_{sub,k} + \sigma^2 I_Q)^{-1} Y_{sub,k} \ , \qquad (17)$$

where $H_{sub,k}$ is the submatrix with the following elements

$$\begin{bmatrix} H^{banded}_{(k-D)_N,(k-2D)_N} & \cdots & H^{banded}_{(k-D)_N,(k+2D)_N} \\ \vdots & \ddots & \vdots \\ \vdots & \ddots & \vdots \\ \vdots & \ddots & \vdots \\ H^{banded}_{(k+D)_N,(k-2D)_N} & \cdots & H^{banded}_{(k+D)_N,(k+2D)_N} \end{bmatrix} , \qquad (18)$$

$(.)_N$ is the modulo-N operation, $h_{sub,k}$ is the middle column of $H_{sub,k}$, $Q = 2D+1$ is the number of filter taps, σ^2 is the noise plus residual ICI power and $Y_{sub,k} = [Y_{(k-D)_N}, ..., Y_{(k+D)_N}]^T$ is the sub-observation vector of dimension $(2D+1)$x1. The residual ICI arises due to the banded approximation, and it can be calculated as a function of D as given by [9, eq.(4)]. $H_{sub,k}$ in (18) has two $2D$x$2D$ zero triangles in the upper-right and lower-left corners. As opposed to [2], these elements are replaced by their corresponding values as the overall complexity remains the same, while improving the performance.

B. Decision Feedback Equalizer

The DFE is a non-linear equalizer, where the hard-decided symbols are fed back to eliminate their interference from the received signal improving the subsequent symbol estimates. The MMSE DFE symbol estimate of subcarrier k is given by

$$\tilde{X}_k = h^H_{sub,k}(H_{sub,k} Q_e H^H_{sub,k} + \sigma^2 I_Q)^{-1} Y^{new}_{sub,k} \ , (19)$$

$$Q_e = \text{diag}\{q_{(k-2D)_N}, ..., q_{(k+2D)_N}\} \ , \qquad (20)$$

where $q_m = 0$ if X_m has been already detected and 1 if not and $Y^{new}_{sub,k}$ is the received signal at subcarriers $(k-D)_N$ to $(k+D)_N$ after cancelling the interference of the previously detected symbols. After passing $\tilde{X}_k$ through the hard decision device, the estimate thereof becomes $\hat{X}_k$, and its interference on its $2D_e$ neighbours is cancelled as follows

$$Y^{new}_{(k-D_e)_N:(k+D_e)_N} = Y^{old}_{(k-D_e)_N:(k+D_e)_N} - H_{(k-D_e)_N:(k+D_e)_N,k} \hat{X}_k \ , (21)$$

here : is a notation for to. The received signal Y is updated after each symbol cancellation. To avoid a high complexity in finding the optimal detection order, only the symbol X_m with the largest norm of $h_{sub,m}$ is computed and the detection order is $X_m, X_{m+1}, ..., X_{N-1}, X_0, ..., X_{m-1}$ [1].

V. ICI Precancellation

The LS pilot estimates in (7) are corrupted by ICI, which lead to inaccuracies in estimating the main diagonal of H. This gives rise to greater inaccuracies in estimating the off-diagonals due to their smaller magnitudes. The estimation of H can be improved by precancelling the ICI of the neighbouring $2D_p$ subcarriers on the IPs used for CE as follows

$$Y^{precancelled}_{IP} = Y_{IP} - \sum_{m=IP-D_p, m \neq IP}^{IP+D_p} \hat{H}_{IP,m} \hat{X}_m \ . \qquad (22)$$

To get the initial symbol estimates for ICI precancellation, a two-stage equalizer is used. Since ICI precancellation strongly depends on the symbol estimates, a two-stage equalizer with an iterative loop as shown in Fig. 2 would yield higher performance gains.

A. LLR Window

To exploit the ICI precancellation gain, the CE IPs are not limited to pilots, but also reliable data symbols from stage 1. As shown in Fig. 3, $Y^{precancelled}$ at positions d1 and d2 would contain less residual ICI in comparison to the pilots, because their closest neighbours can be decided correctly.

An LLR window of size 5 is introduced, which contains the LLR magnitudes of the IP and its closest 4 neigbours, which on average contain 75% of the total ICI power [1]. To optimize the IPs, the LLR window slides over the subcarriers, and the

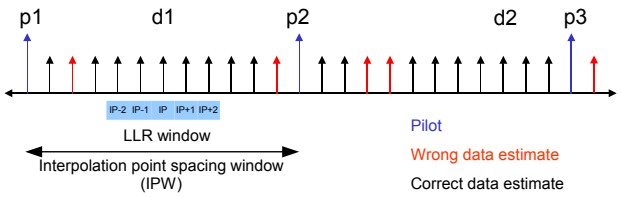

Fig. 3. LLR window approach

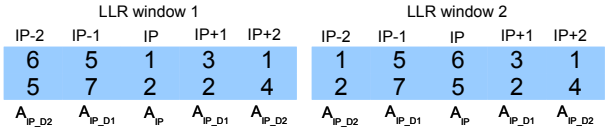

Fig. 4. LLR window example, for M=4 (QPSK)

probability that all the symbols lying in the LLR window are correct is computed as follows

$$P_{c,LLR\_window} = \prod_{symbol=IP-2}^{IP+2} \prod_{bit=1}^{B} P_{c,symbol,bit} \quad (23)$$

$$P_{c,symbol,bit} = \frac{\exp(A_{symbol}|LLR|)}{1+\exp(A_{symbol}|LLR|)} , \quad (24)$$

where $B = log_2 M$ and A_{symbol} is a scaling factor. The IP which maximizes P_{c,LLR_window} inside an interpolation point window (IPW) is chosen. A_{symbol} is introduced to give different priorities to the symbols in the LLR window. The IP is the most important one, because an erroneous IP gives an erroneous LS estimate, followed by the closest two neighbours, because they contain the greatest percentage of ICI power, and the furthest two neighbours are the least important. Without including A_{symbol}, both LLR windows in Fig. 4, where M=4, would give the same P_{c,LLR_window}, although the IP in window 2 is more reliable. In general, the scaling factors should be chosen such that $A_{IP} < A_{IP\_D1} < A_{IP\_D2}$.

Since there are regions in the OFDM symbol with burst errors, due to the frequency selective channel, IPW could be increased if the maximium P_{c,LLR_window} falls below a certain threshold to find a better IP. Using the sampling theorem for a 1D frequency interpolator, the maximum IPW is $\frac{1}{\tau_{max}\Delta f}$, where τ_{max} is the maximum delay [10]. IPW should be a compromise between the interpolation error and P_{c,LLR_window}. As IPW increases, the distance between the IPs and the interpolation error increases, because the IPs' crosscorrelation decreases.

B. Post-Processor

As compared to the LLR window, the best case scenario would be to use the pilots as IPs and correctly detect the 4 neighbours of each pilot, because the pilots are usually boosted (indicated in Fig. 3). As a result, the LS estimate at a pilot would have a smaller variance for the same residual ICI and noise power as compared to a data symbol. Therefore, a PP will be used to improve the estimates of the pilots' neighbours instead of optimizing the IPs. The PP was introduced in [11], where it was used to obtain reliability information on the detected symbols. Y_k after canceling the interference of the $2D_e$ neighbours detected e.g. by MMSE DFE becomes

$$Y_k^{DFE} = Y_k - \sum_{I=k-D_e, I\neq k}^{k+D_e} \hat{H}_{k,I}\hat{X}_I \ . \quad (25)$$

The maximum-likelihood (ML) is given by

$$P(Y_{sub,k}|X_k) = \frac{1}{(2\pi\sigma^2)^{2D+1}} e^{-\frac{|Y_{sub,k}-\hat{h}_{sub,k}X_k|^2}{2\sigma^2}} , \quad (26)$$

where $Y_{sub,k} = [Y^{DFE}_{(k-D)_N}, ..., Y^{DFE}_{(k+D)_N}]^T$ and $\hat{h}_{sub,k}$ is the estimated $h_{sub,k}$. X_k is permuted and the constellation point maximizing the ML is chosen. The complexity is greatly reduced in comparison with the optimal ML detector, since the other $4D$ symbols contributing to $Y_{sub,k}$ are not permuted. The unreliable bits of the $4D$ symbols can also be permuted at an additional complexity. The improved estimates of the pilots' neighbours reduce the ICI on the pilots at the ICI precancellation stage improving CE.

VI. Simulation Results

The simulation parameters are shown in Table I. The channel model used is the COST207 6-tap Typical Urban (TU6) [12]. The pilot pattern used is PP1 as defined in the DVB-T2 specification [13], where the scattered and continual pilots have boosting factors of $4/3$ and $8/3$, respectively. Stage 1 in Fig. 2 is a 7 taps MMSE FEQ, stage 2 is a 3 taps MMSE DFE, and the Wiener filter has $N_{taps} = 4$. D_e and D_p are equal to 10 and D used by the PP in (26) is equal to 3. The scaling factors of the LLR window were empirical optimized, where $A_{IP} = 0.6$, $A_{IP\_D1} = 0.8$, and $A_{IP\_D2} = 1$. The IPW length is equal to the pilot spacing but is extended to double its length if the maximum P_{c,LLR_window} falls below 0.9. IPWs larger than double the pilot spacing yield less reliable CE, since the correlation between the IPs decreases.

Fig. 5 shows the performance of the two iterative ICI precancellation schemes discussed in comparison to the 3 taps DFE without ICI precancellation at an SNR of 40 dB. We focus on such high SNR to analyze the effect of ICI mitigation, where ICI dominates noise, and to investigate the inherent error floors from residual ICI. Genie-directed ICI precancellation corresponds to the case where only the pilots are used as IPs and estimated symbols from stage 1 are cancelled only if they are correct, i.e. wrong ICI precancellation is avoided. The performance of the LLR window scheme approaches the genie-directed case after the first iteration, and it has a gain of appproximately 80 Hz in f_{dmax} at a target symbol error rate (SER) of 10^{-3} compared to the DFE without ICI precancellation, which corresponds to more than 0.07 increase in f_{dnorm}. The LLR window approach outperforms the PP by optimizing the IPs.

The SER is also compared versus SNR at f_{dnorm} of 10%

TABLE I
SIMULATION PARAMETERS

Parameter	value
FFT size	8192
Active subcarriers	6817
Subcarrier spacing	1116 Hz
Cyclic prefix	1/4
Modulation	QPSK
Pilot spacing	12

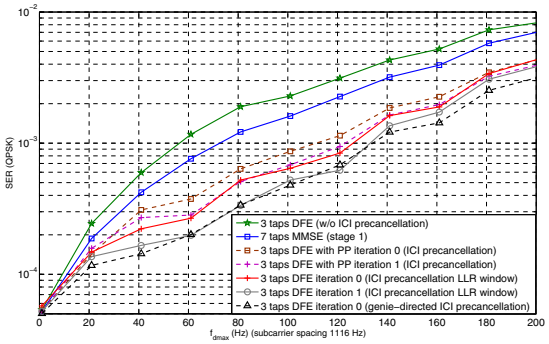

Fig. 5. SER versus f_{dmax} at SNR 40 dB

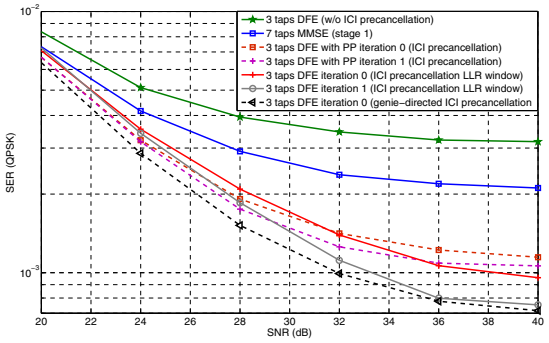

Fig. 6. SER versus SNR at $f_{dnorm} = 0.1$

and 15% in Figs. 6 and 7, respectively. For DVB-T2 system with $f_c = 600$ MHz, f_{dnorm} of 10% and 15% correspond to user velocties of 200 km/h and 300 km/h, respectively. As the SNR decreases, the ICI power does not become the dominant source of error; therefore, the PP becomes better than the LLR window scheme due to the boosting factor of the pilots. As expected at 15% f_{dnorm}, the LLR window scheme gets better than the PP at already a lower SNR as compared to 10% f_{dnorm}, because the ICI power is greater. Even the genie-directed case approaches the same performance as the other equalizers at low SNR due to the noise dominance. At low SNR, error floors due to ICI are interesting for coded systems, where forward error correction may resolve error floors down to a particular threshold. The 3 taps DFE exhibits an unacceptably high error floor without ICI precancellation, and it outperforms the 7 taps MMSE FEQ after ICI precancellation. The performance of the iterative ICI precancellation converges after more iterations.

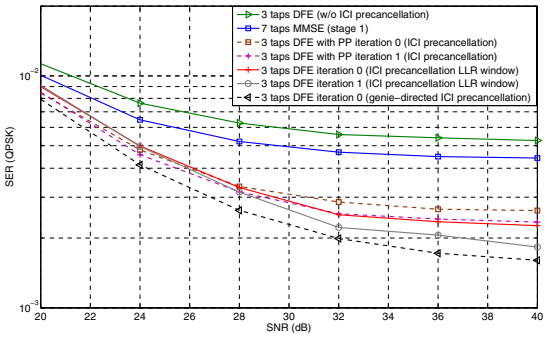

Fig. 7. SER versus SNR at $f_{dnorm} = 0.15$

VII. CONCLUSION

We proposed two methods for ICI precancellation to improve the FD CE. The ICI precancellation gain is exploited in the first method by optimizing the IPs used for CE, while in the second method by improving the estimates of the pilots' neighbours. The first method shows a better performance when the ICI power is dominant, and the second method is better when the noise and ICI powers are comparable due to the boosting factor of the pilots. Significant performance gains were achieved by the DFE after ICI precancellation with only one iteration supporting an increase of 0.07 in f_{dnorm}.

REFERENCES

[1] X. Cai and G. Giannakis, "Bounding Performance and Suppressing Intercarrier Interference in Wireless Mobile OFDM," *IEEE Trans. Commun.*, vol. 51, no. 12, 2003.

[2] S. Lu, R. Kalbasi, and N. Al-Dhahir, "OFDM Interference Mitigation Algorithms for Doubly-Selective Channels," *IEEE 64th Veh. Technol. Conf.*, 2006.

[3] A. Gorokhov and J. Linnartz, "Robust OFDM Receivers for Dispersive Time-Varying Channels: Equalization and Channel Acquisition," *IEEE Trans. Commun.*, vol. 52, no. 4, Apr. 2004.

[4] S. Lu and N. Al-Dhahir, "Coherent and Differential ICI Cancellation for Mobile OFDM with Application to DVB-H," *IEEE Trans. Wireless Commun.*, vol. 7, no. 7, Jul. 2008.

[5] C. Hsu and W. Wu, "Low-Complexity ICI Mitigation Methods for High-Mobility SISO/MIMO-OFDM Systems," *IEEE Trans. Veh. Technol.*, vol. 58, no. 6, Jul. 2009.

[6] K. Kwak, S. Lee, H. Min, S. Choi, and D. Hong, "New OFDM Channel Estimation with Dual-ICI Cancellation in Highly Mobile Channel," *IEEE Trans. Wireless Commun.*, vol. 9, no. 10, Oct. 2010.

[7] H. Hijazi and L. Ros, "Polynomial Estimation of Time-Varying Multipath Gains With Intercarrier Interference Mitigation in OFDM Systems," *IEEE Trans. Veh. Technol.*, vol. 58, Jan. 2009.

[8] Y. Mostofi and D. Cox, "ICI Mitigation for Pilot-Aided OFDM Mobile Systems," *IEEE Trans. Wireless Commun.*, vol. 4, no. 2, Mar. 2005.

[9] M. Muenster and L. Hanzo, "Second-order Channel Parameter Estimation Assisted Cancellation of Channel Variation-induced Inter-subcarrier Interference in OFDM systems," *Proc. Int. Conf. EUROCON 21*, vol. 1, Jul. 2001.

[10] P. Hoeher, S. Kaiser, and P. Robertson, "Two-Dimenstional Pilot-Symbol-Aided Channel Estimation By Wiener Filtering," in *Proc. IEEE Int. Symp. Inf. Theory*, Jul. 1997.

[11] N. Seshardi and P. Hoeher, "On Post-Decision Symbol-Reliability Generation," *IEEE Int. Conf. Commun., 1993*, vol. 2, May 1993.

[12] C. . WG1, "Proposal on channel transfer functions to be used in GSM Tests late 1986," CEPT Paris, Tech. Rep., Sep. 1986.

[13] ETSI, "ETSI EN 302 755 v1.1.1, Digital Video Broadcasting (DVB); Frame structure channel coding and modulation for a second generation digital terrestrial television broadcasting system (DVB-T2)," Tech. Rep., Sep. 2009.